


 Cite this: *RSC Adv.*, 2017, **7**, 49532

 Received 12th July 2017  
 Accepted 13th October 2017

 DOI: 10.1039/c7ra07671a  
[rsc.li/rsc-advances](http://rsc.li/rsc-advances)

## Monothiatruxene: a new versatile core for functional materials†

 Michał R. Maciejczyk, <sup>\*ac</sup> J. A. Gareth Williams, <sup>b</sup> Neil Robertson, <sup>\*c</sup> and Marek Pietraszkiewicz<sup>a</sup>

A truxene molecule incorporating a sulfur atom at one of the three bridgehead positions has been prepared through an efficient route, together with its oxidized analogue (featuring an  $\text{SO}_2$  unit) and brominated derivatives. The photophysical, electrochemical and thermal properties of the compounds are presented: the materials show high thermal stability and the ability to form amorphous glasses. This central monothiatruxene core offers multiple routes to further modifications, thereby opening a way to the synthesis of a variety of novel functional materials beyond the parent truxene.

10,15-Dihydro-5H-diindeno[1,2-*a*;1',2'-*c*]fluorene – commonly known as truxene – is a planar heptacyclic polyarene structure obtained by trimerization of indan-1-one, originally reported in 1887.<sup>1</sup> It can be considered as three fused fluorene moieties. Analogues incorporating sulfur, oxygen or nitrogen in place of the  $\text{CH}_2$  at the bridgehead positions – namely trithiatruxene, trioxatruxene and triazatruxene, respectively – can similarly be thought of as built up from fused dibenzothiophene, dibenzofuran and carbazole units. Truxene has recently attracted a lot of attention in organic electronics due to a desirable combination of properties such as exceptional solubility, high thermal stability and ease of modification.<sup>2,3</sup> Consequently, it has been used as a material for two-photon absorption,<sup>4</sup> organic light emitting diodes (OLEDs),<sup>5-7</sup> organic field effect transistors (OFETs),<sup>8,9</sup> organic solar cells (OSCs),<sup>10</sup> dye-sensitized solar cells (DSSCs)<sup>11,12</sup> and organic lasers.<sup>13</sup> On the other hand, trithiatruxene, due to its difficult synthesis and poor solubility, has largely been utilized only as a discotic mesogen<sup>14</sup> in liquid crystal displays.<sup>15</sup>

Here, we have sought to essentially merge the properties of truxene and trithiatruxene (Fig. 1), *via* a novel, straightforward synthetic route to monothiatruxene (**TrxS**), a material that had previously been only briefly reported in the patent literature.<sup>16,17</sup> We go on to show that monothiatruxene can be used as a platform for diverse structural modification.

Target materials monothiatruxene (**TrxS**) and monosulfonyltruxene (**TrxSO<sub>2</sub>**) were synthesized through a stepwise

synthetic route starting from 1,3,5-tris-(2'-bromophenyl)benzene, as presented in Scheme 1.

The first step, which is a selective substitution of one bromine with methyl sulfide group through lithiation, must be performed at low temperature over at least 1 h in order to form the most stable lithiated species,<sup>18</sup> namely the selectively monosubstituted product. To the lithiated substrate, dimethyl disulfide was introduced as a source of sulfur. The pendent sulfur was then oxidized and subsequent ring closure achieved with the aid of acid according to known methods used for the synthesis of dibenzothiophenes.<sup>19</sup> Lithiation at the remaining bromine sites followed by addition of pentan-3-one gave the dialcohol **4** in a satisfactory yield of 54%; the limit on yield may be caused by enolization of the ketone in the presence of alkylolithium reagents. Condensation and cyclisation of **4** works best by using Lewis acids, especially boron trifluoride etherate, giving the expected monothiatruxene product (**TrxS**) within minutes after the addition of the  $\text{BF}_3$  reagent, with a high yield of 85%. The monothiatruxene (**TrxS**) can be easily transformed to the *S,S*-dioxide (**TrxSO<sub>2</sub>**) upon treatment with hydrogen peroxide in acetic acid, with a yield of 60% yield.

The final monothiatruxene (**TrxS**) can be easily modified (Scheme 2) to serve as a versatile platform for functional materials, similarly to the parent truxene molecule. The scheme shows a few examples of derivatization that have been accomplished,

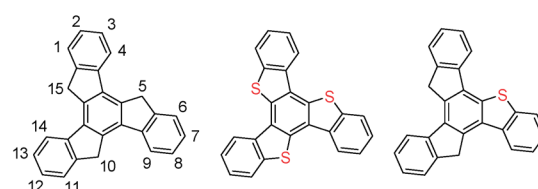


Fig. 1 Structures of truxene, trithiatruxene and monothiatruxene.

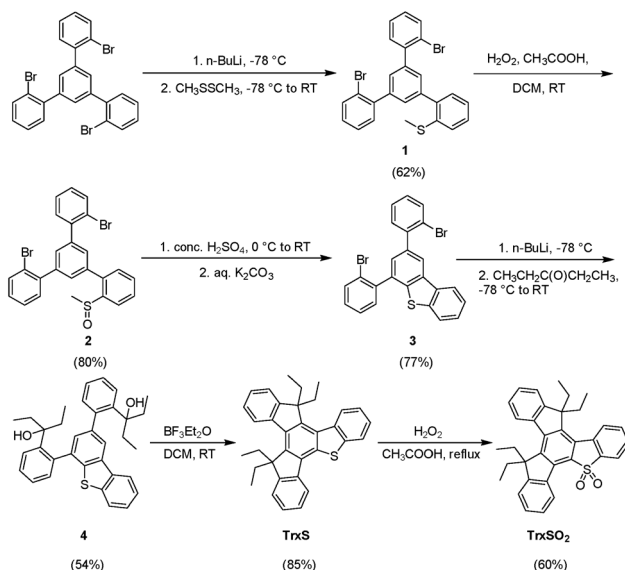
<sup>a</sup>Institute of Physical Chemistry, Polish Academy of Sciences, Kasprzaka 44/52, Warsaw, 01-224, Poland

<sup>b</sup>Department of Chemistry, Durham University, South Road, Durham DH1 3LE, UK

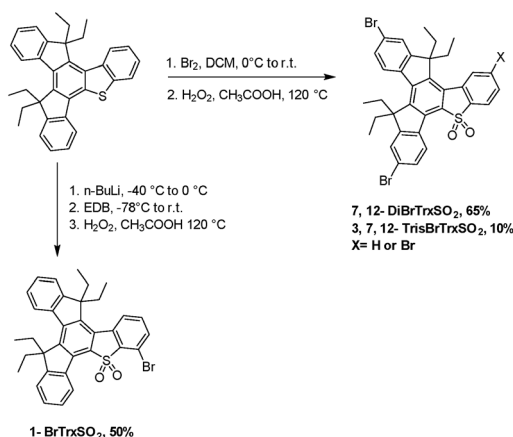
<sup>c</sup>EaStCHEM School of Chemistry, University of Edinburgh King's Buildings, Edinburgh EH9 3FL, UK. E-mail: [m.maciejczyk@ed.ac.uk](mailto:m.maciejczyk@ed.ac.uk); [neil.robertson@ed.ac.uk](mailto:neil.robertson@ed.ac.uk)

† Electronic supplementary information (ESI) available: Experimental procedures and  $^1\text{H}$ ,  $^{13}\text{C}$ , 2D NMR and MS data for all new compounds. UV-VIS spectra, SWV traces, XRD patterns, DSC and TGA scans for compounds **TrxS** and **TrxSO<sub>2</sub>**. See DOI: 10.1039/c7ra07671a





Scheme 1 Synthetic route to monothiatruxene.



Scheme 2 Derivatization of monothiatruxene.

involving introduction of bromine atoms into different positions, and sulfur oxidation.

Selective bromination of the aromatic ring adjacent to the sulfur atom (position 1) has been achieved by *ortho*-lithiation and subsequent treatment with 1,2-dibromoethane. Di- and tri-brominated derivatives were obtained with the use of simple bromination method with the use of bromine in dichloromethane. Non-oxidized intermediates, namely **1-BrTrxS**, **7,12-DiBrTrxS** and **3,7,12-TrisBrTrxS**, were directly subjected to oxidation with hydrogen peroxide. The tribrominated product appeared as a side product of the reaction aiming for the dibromo derivative therefore the final yield is only 10%. Where the aimed **7,12-DiBrTrxSO<sub>2</sub>** has been obtained in 65% yield. The **1-BrTrxSO<sub>2</sub>** was obtained in 50% yield, after three steps; *ortho*-lithiation, reaction with ethylene dibromide and oxidation with hydrogen peroxide. All obtained materials possess good solubility in most common organic solvents even though only ethyl chains were utilized. Detailed reaction descriptions can be

found in the ESI.† All the materials were fully characterized by <sup>1</sup>H, <sup>13</sup>C and 2D NMR spectroscopy and mass spectrometry. Final materials were also characterized by elemental analysis.

The UV-VIS absorption and fluorescence spectra of **TrxS** and **TrxSO<sub>2</sub>** in dilute dichloromethane solution are presented in Fig. 2. The corresponding spectra in cyclohexane and acetonitrile (less and more polar solvents than CH<sub>2</sub>Cl<sub>2</sub> respectively) were almost identical, showing no significant solvatochromism (Fig. S1†). Both compounds absorb light only in the UV region with  $\lambda_{\text{max}}$  288 nm ( $\epsilon = 54\,800\text{ cm}^{-1}\text{ M}^{-1}$ ) and 285 nm ( $\epsilon = 35\,000\text{ cm}^{-1}\text{ M}^{-1}$ ) for **TrxS** and **TrxSO<sub>2</sub>**, respectively, with somewhat weaker absorption peaks at longer wavelength: 350 and 366 nm for **TrxS** and 357 and 374 nm for **TrxSO<sub>2</sub>**. The emission bands appear at only slightly lower energy than the lowest-energy absorption bands: the Stokes shifts are only 550 cm<sup>-1</sup> for **TrxS** and 940 cm<sup>-1</sup> for **TrxSO<sub>2</sub>**. This contrasts with unsubstituted hexaalkyltruxene, which has a large Stokes shift of 4600 cm<sup>-1</sup>. Clearly,  $C_{3h}$  symmetry-forbidden transitions in truxene<sup>20</sup> become allowed upon introduction of the sulfur atom to the core, accounting for the small Stokes shifts. In Fig. S2,† the mirror image relationship between the absorption and emission bands can be observed for both materials. Oxidation of the sulfur atom leads to a less structured spectral profile and red-shifting of the emission maximum: a red-shift of 830 cm<sup>-1</sup> in **TrxSO<sub>2</sub>** compared to **TrxS** (580 cm<sup>-1</sup> in the lowest energy absorption band). The fluorescence quantum yield ( $\Phi_{\text{fl}}$ ) of **TrxS** is 0.05, while oxidation to **TrxSO<sub>2</sub>** increases this value to 0.14. Table 1 summarizes the photophysical and thermal data.

The oxidation and reduction potentials were obtained from square-wave voltammetry (SWV) experiments using ferrocene as an internal standard (Fig. S3†). Only one oxidation peak of **TrxS** was recorded at 0.86 V and no reduction. In contrast, **TrxSO<sub>2</sub>** showed only one reduction peak at -2.21 V without oxidation under the same conditions. Both oxidation of **TrxS** and reduction of **TrxSO<sub>2</sub>** remain unchanged with the scan direction (Fig. S4†). The cyclic voltammetry measurement (Fig. 3) at five different scan rates showed that **TrxS** can be stably and reversibly oxidized (Fig. 3, S5 and Table S1†). The cathodic/anodic current ratio is about 1, proving the stability of the oxidized species.

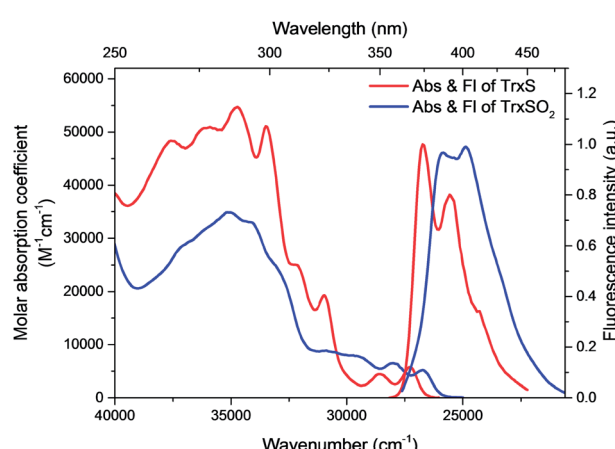
Fig. 2 Absorption and fluorescence spectra of **TrxS** and **TrxSO<sub>2</sub>** in dichloromethane solution.

Table 1 Electrochemical, photophysical and thermal properties

|                          | $\lambda_{\text{abs}}^a, \text{nm}$ | $\epsilon^a \times 10^3, \text{cm}^{-1} \text{M}^{-1}$ | $\lambda_{\text{fl}}^a, \text{nm}$ | Stokes shift <sup>a</sup> , $\text{cm}^{-1}$ | $E_{\text{gap}}^{a,b}, \text{eV}$ | $\Phi_{\text{fl}}^{a,c}$ | $E_{\text{ox}}^a, \text{V}$ | $E_{\text{red}}^a, \text{V}$ | $T_g^d, {}^\circ\text{C}$ | $T_m^d, {}^\circ\text{C}$ | $T_d^e, {}^\circ\text{C}$ |
|--------------------------|-------------------------------------|--|------------------------------------|--|-----------------------------------|--------------------------|-----------------------------|------------------------------|---------------------------|---------------------------|---------------------------|
| <b>TrxS</b>              | 288, 299,<br>350, 366               | 54.8, 51.1,<br>4.5, 5.7                                | 374, 391                           | 550  | 3.38                              | 0.05                     | +0.86                       | —                            | 84                        | 208, 214                  | 326                       |
| <b>TrxSO<sub>2</sub></b> | 285, 357, 374                       | 35, 6.5, 5.2   | 387, 400                           | 940  | 3.42                              | 0.14                     | —                           | -2.21                        | 119                       | 256                       | 357                       |

<sup>a</sup> In dichloromethane solution. <sup>b</sup> Optical gap, from intersection of Abs and Pl. <sup>c</sup> In reference to quinine sulfate in 0.1 N H<sub>2</sub>SO<sub>4</sub> ( $\Phi = 0.51$ ). <sup>d</sup> Glass transition temperature ( $T_g$ ) and melting point ( $T_m$ ) by DSC. <sup>e</sup> Decomposition temperature ( $T_d$ ) by TGA.

Therefore, it may be concluded that this redox couple is reversible. On the other hand, the reversibility of the reduction of the **TrxSO<sub>2</sub>** could not be evaluated, as can be seen in the Fig. 3, since the process is close to the solvent window and both peaks could not be distinguished clearly.

The differential scanning calorimetry (DSC) showed that both materials are of crystalline nature with melting points of 198 °C and 214 °C for **TrxS** and 256 °C for **TrxSO<sub>2</sub>** (see Fig. S6 and S7†). After melting the material and heating it again, **TrxS** showed a glass transition temperature of 84.5 °C and cold crystallization at 180.6 °C along with again two melting points at 207.8 °C and

213.7 °C. **TrxSO<sub>2</sub>** showed on the second heating a glass transition at 119.3 °C but no cold crystallization and only a tiny peak representing melting point indicating that the material is mostly amorphous. Additionally, powder diffraction patterns confirmed the crystalline nature of both as-synthesized truxenes (Fig. S8†) in their powder form. Thermogravimetric analysis proved the high thermal stability of **TrxS** with 5% mass loss at the temperature of 326 °C and for **TrxSO<sub>2</sub>** 357 °C (Fig. S6 and S7†) which can be attributed to the all-aromatic backbone. Both DSC and TGA show how the introduction of oxygen atoms affects thermal properties where the melting point and glass transition temperature increase. Moreover, the sulfonyl group probably prevents stacking of the rings and leads to a more stable amorphous state. All these indicate that monothiatruxenes are promising candidates for optoelectronic applications.

In conclusion, we designed and synthesized monothiatruxene, its oxidized derivative and their brominated counterparts. The presented work shows that introduction of a sulfur atom to the truxene structure affects its electronic properties while maintaining high thermal stability. Additionally, due to the low symmetry of the molecule and presence of sulfur, a wider range of modifications is possible than that for truxene. Importantly, these materials also show high solubility.

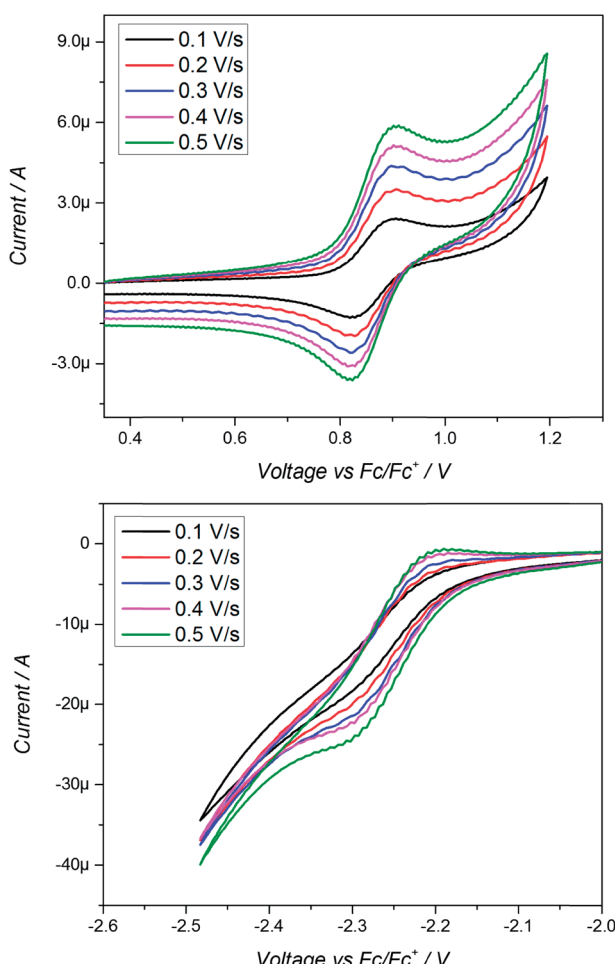


Fig. 3 Cyclic voltammograms of **TrxS** (top) and **TrxSO<sub>2</sub>** (bottom) at different scan rates.

## Author contributions

The manuscript was written through contributions of all authors. All authors have given approval to the final version of the manuscript.

## Conflicts of interest

There are no conflicts to declare.

## Acknowledgements

We thank the International PhD Projects Programme of the Foundation for Polish Science, co-financed from European Regional Development Fund within Innovative Economy Operational Programme “Grants for innovation” (MPD-A1) and European Union’s Horizon 2020 Research and Innovation Programme H2020-MSCA-IF-2014-659237 for financial support. We thank Krzysztof Górska for helpful discussions.



## References

- 1 W. Wislicenus, *Ber. Dtsch. Chem. Ges.*, 1887, **20**(1), 589.
- 2 F. Goubard and F. Dumur, *RSC Adv.*, 2015, **5**(5), 3521.
- 3 G. Zhang, F. Rominger and M. Mastalerz, *Chem.-Eur. J.*, 2016, **22**(9), 3084.
- 4 Y. Xie, X. Zhang, Y. Xiao, Y. Zhang, F. Zhou, J. Qi and J. Qu, *Chem. Commun.*, 2012, **48**(36), 4338.
- 5 X.-Y. Cao, X.-H. Liu, X.-H. Zhou, Y. Zhang, Y. Jiang, Y. Cao, Y.-X. Cui and J. Pei, *J. Org. Chem.*, 2004, **69**(18), 6050.
- 6 Z. Yang, B. Xu, J. He, L. Xue, Q. Guo, H. Xia and W. Tian, *Org. Electron.*, 2009, **10**(5), 954.
- 7 M. Kimura, S. Kuwano, Y. Sawaki, H. Fujikawa, K. Noda, Y. Taga and K. Takagi, *J. Mater. Chem.*, 2005, **15**(24), 2393.
- 8 Y. M. Sun, K. Xiao, Y. Q. Liu, J. L. Wang, J. Pei, G. Yu and D. B. Zhu, *Adv. Funct. Mater.*, 2005, **15**(5), 818.
- 9 X. R. Zhang, W. Chao, Y. T. Chuai, Y. Ma, R. Hao, D. C. Zou, Y. G. Wei and Y. Wang, *Org. Lett.*, 2006, **8**(12), 2563.
- 10 Z. Lu, C. Li, T. Fang, G. Li and Z. Bo, *J. Mater. Chem. A*, 2013, **1**(26), 7657.
- 11 X. Zong, M. Liang, C. Fan, K. Tang, G. Li, Z. Sun and S. Xue, *J. Phys. Chem. C*, 2012, **116**(20), 11241.
- 12 X. Qian, Y. Z. Zhu, J. Song, X. P. Gao and J. Y. Zheng, *Org. Lett.*, 2013, **15**(23), 6034.
- 13 G. Tsiminis, Y. Wang, P. E. Shaw, A. L. Kanibolotsky, I. F. Perepichka, M. D. Dawson, P. J. Skabar, G. A. Turnbull and I. D. W. Samuel, *Appl. Phys. Lett.*, 2009, **94**(24), 243304.
- 14 R. Cayuela, H. T. Nguyen, C. Destrade and A. M. Levelut, *Mol. Cryst. Liq. Cryst.*, 1989, **177**(1), 81.
- 15 Y. Kobori, T. Toyooka, H. Mazaki and Y. Satoh, US 5855971, 1996.
- 16 M. Maciejczyk, K. Górska and M. PietraszkiewiczPL407006, 2014.
- 17 S. Y. Hyun, Y. H. Yoon and J. H. Song, KR20140000611, 2014.
- 18 J. Clayden, *Organolithiums: Selectivity for Synthesis*, Pergamon, 2002.
- 19 V. Pandya, M. Jain, B. V. Chaugule, J. S. Patel, B. M. Parmar, J. K. Joshi and P. R. Patel, *Synth. Commun.*, 2012, **42**(4), 497.
- 20 M.-T. Kao, J.-H. Chen, Y.-Y. Chu, K.-P. Tseng, C.-H. Hsu, K.-T. Wong, C.-W. Chang, C.-P. Hsu and Y.-H. Liu, *Org. Lett.*, 2011, **13**(7), 1714.

